Marcus Scheele

FOR WHAT IT'S WORTH: LONG-RANGE ORDER AND ORIENTATION IN NANOCRYSTAL SUPERLATTICES

1. INTRODUCTION

In 1995, a very important paper was published, detailing the self-assembly of small crystallites of the semiconductor CdSe into a three-dimensional superstructure with long-range order and domain sizes of up to 50 µm.[1] Since each crystallite consists of just several thousand atoms spanning a diameter of under 5 nm, a single domain of the three-dimensional superstructure contains many millions of these nanocrystals (NC). In analogy to classical crystals which are ordered arrays of atoms, such three-dimensional superstructures are referred to as "superlattices", in which the NCs function as "quasi-atomic" building blocks. The analogy to atoms continues as many semiconductor nanocrystals are small enough to fall into the large quantum confinement regime, such that they exhibit discrete, atom-like electronic states.[2] Since this seminal paper, an overwhelming structural diversity of NC superlattices has been reported, which has not only been an aesthetically pleasing Eldorado for electron microscopists and crystallographers but also frequently served to reiterate the term "quasi-atoms", including the associated expectations for future applications of NC superlattices as novel electronic materials with emergent properties.[3] A quarter of a century later, it appears justified to ask whether these expectations were realistic and whether they may be met in the near future. Does structural order and orientation in NC superlattices really matter in that it significantly changes the optoelectronic properties of the array compared to a disordered ensemble of the same NCs? What are the chemical challenges that can prevent the emergence of novel physical properties by design of the structure of a superlattice? This short perspective addresses these questions and provides recent examples to illustrate the state-of-the-art of self-assembled NC superlattices with emergent optoelectronic functionalities.

Dr. Marcus Scheele
Institute of Physical and Theoretical Chemistry
Universität Tübingen
Auf der Morgenstelle 18, 72076 Tübingen
Tel.: +49 7071/29-76243, Telefax: +49 7071/29-5490
E-Mail: marcus.scheele@uni-tuebingen.de
www.uni-tuebingen.de/COIN
DOI: .....

2. CHALLENGES WITH EXPLOITING THE EMERGENT OPTOELECTRONICS OF NANOCRYSTAL SUPERLATTICES

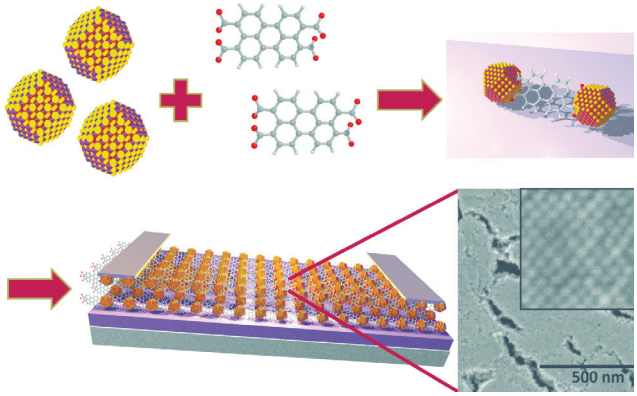

Figure 1. Idealized schematics of the self-assembly of inorganic NCs and organic π-systems into hybrid superlattices, in which adjacent NCs are cross-linked by the conjugated π-systems for better electronic coupling. The electron micrograph shows the high degree of structural order in typical superlattices.

Time-resolved spectroscopy and X-ray scattering have revealed that a larger degree of structural order in NC ensembles improves the carrier hopping rate.[4] This is consistent with computational studies, which predicted that the coupling between NCs strongly depends on their shape and orientation to each other.[5, 6] One hypothesis developed in these simulations was that anisotropic transport properties should arise due to differences in the coupling for electrons vs. holes between two NCs.[6–8]

In order to apply NC superlattices in electronic devices, a chemistry had to be developed which not only establishes long-range order and orientation in the superlattices, but also electronic coupling between the constituting NCs. The organic ligand shell that stabilizes colloidal NCs in solution has a detrimental effect on the coupling between the particles, rendering the superlattice self-assembled from such NCs electrically insulating. A common strategy to overcome this effect is exchanging the native ligand shell with shorter ligands, which indeed enhances the NC-NC coupling and, thus, the electrical conductivity and charge carrier mobility.[9] However, this ligand exchange creates cracks and voids, caused by reducing the interparticle distances, which breaks the structural long-range order of the NC assembly.[10, 11] An alternative strategy – based on ligand exchange with organic π-systems, such as metal tetraaminophthalocyanines or perylenes, can mitigate this problem and

create conductive NC superlattices with long-range order (Figure 1).[12] This enables an experimental verification of emergent electronic properties like anisotropic charge transport in NC superlattices, which I will address after a short account of some fundamental theoretical considerations.

3. THEORY OF TRANSPORT IN SUPERLATTICES OF SEMICONDUCTOR NANOCRYSTALS

Recent investigations have shown that transport in many NC ensembles is best described by an adaption of Holstein's small polaron hopping model.[8, 13] Polar semiconductors (e.g. CdSe or PbS) exhibit strong coupling between charge carriers and optical phonons which results in the formation of small polarons. The binding energy of such polarons is given by half the Marcus' reorganization energy (λ).[14] If λ is larger than the coupling energy between adjacent NCs, polaron localization takes place: the charge carrier is trapped by the optical phonon and may propagate only via polaronic hopping with the polaronic hopping rate (τ_{Pol}^{-1}) according to Marcus's theory

$$\tau_{Pol}^{-1} = \frac{\epsilon^2}{\hbar}\sqrt{\frac{\pi}{k_B T \lambda}}\exp\left(-\frac{(\lambda+\Delta V)^2}{4\lambda k_B T}\right), \qquad (1)$$

with ∈ the electronic coupling between neighboring NCs, Boltzmann's constant k_B and the height of the potential barrier between adjacent NCs ΔV. [15] Typical reorganization energies (λ) are in the range of 10s to 100s meV, which compare to electronic coupling energies between 1-20 meV, thus validating the assumption of polaron localization on individual NCs (Figure 2a). [8, 16] This localization triggers a surface reconstruction of the NC, during which the bond length between surface atoms and surface ligands of the NC are altered to stabilize the polaron. [8] The propagation of such a polaron through an ensemble of NCs is believed to occur via electrostatic interactions between the charge carriers and the (often) anionic surface ligands of the NCs.[8] This has an important consequence: because the density of the surface molecules can vary substantially for different facets,[17] the electrostatic interaction potential with the injected charge carriers will be facet-specific. For instance, in PbS NCs the binding constant for oleic acid on the {111} facets is roughly 10^6 larger than on the {100} facets (Figure 2b+c). [17] This is consistent with the calculation of a roughly ten times larger coupling energy of polarons along the family of {100} directions vs. the {111} directions (Figure 2a).[8] If polaronic coupling depends on the crystalline direction, one can expect that the polaronic hopping in NC ensembles should become direction-dependent, provided that the ensemble exhibits long-range orientational order. Furthermore, if the NC ensemble is a superlattice with long-range structural order, an additional origin of charge transport anisotropy are direction-dependent interparticle distances. For instance, in a superlattice with body-centered cubic structure, the shortest interparticle distance is along the family of {111} directions. For any other direction of the superlattice, the interparticle distance will be larger, and this decreases polaronic coupling as calculated by Yazdani et al (Figure 2d).[8] Therefore, similar to naturally occurring anisotropic materials like graphene or black phosphorus, NC superlattices with long-range order and iso-orientation of all constituting NCs cloud exhibit charge transport anisotropy. Such superlattices are called "mesocrystals", and the next section will provide a short summary of their fundamental properties.[18]

4. MESOCRYSTALLINE NANOCRYSTAL SUPERLATTICES

Mesocrystals are three-dimensional arrays of iso-oriented single-crystalline particles with an individual size between 1 – 1000 nm.[18, 19] Mesocrystals play an important role in biology, where their extraordinary structure determines the properties of bones, teeth and sea urchin spines to name only a few examples. Their physical properties are largely determined by structural coherence, for which the angular correlation between their individual atomic lattices and the underlying superlattice of NCs is a key feature. A convenient way to investigate this angular correlation is to measure the X-ray scattering pattern of the mesocrystals from the superlattice (at small angles) and from the atomic lattices of the constituting NCs (at large angles) simultaneously. (Figure 3a).[20, 21] Angular X-ray cross-correlation analysis (Figure 3b) is a powerful tool to analyse the angular correlations contained in such datasets and ultimately resolve the full mesocrystalline unit cell, which not only contains the structural information of the superlattice but also the precise orientation of all NCs therein (Figure 3c).[22]

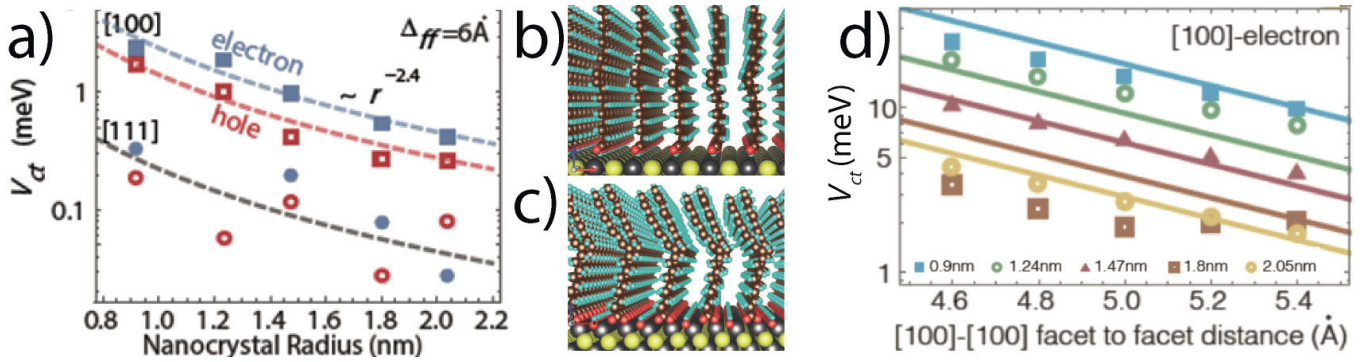

Figure 2. a) Calculated electronic coupling for electrons (blue) or holes (red) between [100] (squares) and [111] (circles) nearest neighbors in PbS NC superlattices with a nearest neighbor distance of 6 Å as a function of the NC radius. b) Relaxed configuration of oleic acid ligands on the PbS(001) surface c) and on the PbS(111) surface. d) Computed electronic coupling for electrons in the [100] direction as a function of the interparticle distance. Different symbols indicate different NC radii. (Figures a+d reprinted from ref. [8] (arXiv:1909.09739). Figures b+c adapted with permission from ref. [17]. Copyright (2014) American Association for the Advancement of Science.)

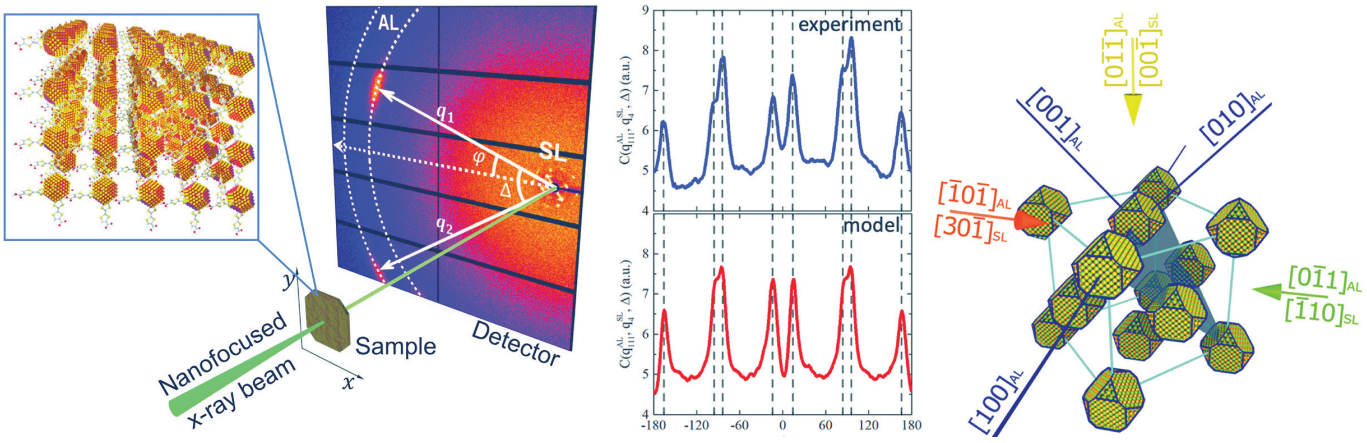

Figure 3. a) Scheme of the diffraction experiment, in which small angle scattering from the mesocrystal superlattice and wide angle scattering from PbS atomic scattering were recorded simultaneously by a large 2D detector. b) Experimentally measured and modelled cross-correlation functions are shown by blue and red color, respectively. (Adapted with permission from ref. [20a]. Copyright (2017) American Chemical Society.) c) A mesocrystalline unit cell for PbS NC superlattices, obtained by angular X-ray cross-correlation analysis of the scattering experiment. Orange, yellow and green arrows indicate colinear crystalline directions of the superlattice (SL) and the atomic lattices of all NCs (AL). (Adapted with permission from ref. [21]. Copyright (2019) WILEY-VCH.)

The ability to assemble electrically conductive NCs into mesocrystalline superlattices and resolve their structure as well as angular correlation now allows to test the computational prediction of anisotropic transport by experiment. One challenge to be overcome to this end is the small domain size of many mesocrystalline NC assemblies, which is often limited to few 10s μm². [11, 21] This limitation is predominantly the result of the surface ligand exchange, which introduces inhomogeneities in the surface coverage as well as the interparticle distance, invokes strain of the superlattice and ultimately the formation of grain boundaries. The footprint of most X-ray-based experiments is larger than these grain sizes, which prohibits the collection of diffraction patterns from single(-crystalline) mesocrystal domains. Here, transmission electron microscopy would unarguably provide a viable alternative, but the need for a thick, mechanically durable substrate which allows contacting the NC assemblies to close an electric circuit for simultaneous transport measurements renders transmission electron microscopy impracticable for this purpose. Advances in X-ray optics and improved coherence of synchrotron light sources have recently made it possible to focus X-ray beams to diameters of several 100 nm and even below, giving access to “X-ray nanodiffraction”, which effectively solves the challenge of imaging single mesocrystalline domains.

5. TRANSPORT ANISOTROPY IN MESOCRYSTALLINE PbS NANOCRYSTAL SUPERLATTICES

Owing to the afore-mentioned advances, the first experimental correlation of mesocrystalline structure and electric conductivity in PbS NC superlattices has now been realized.[23] Single-crystalline mesocrystals could be contacted by lithographically patterned micro-electrodes. Exchanging the insulating oleic acid molecules on the surface of the NCs with the conjugated organic π-system copper β-tetraaminophthalocyanine afforded electrically conductive superlattices. With X-ray nanodiffraction and angular X-ray cross-correlation analysis, the structure of the superlattice and its orientation with respect to the applied electric field were determined. The striking result of this work is that charge transport is more efficient if the nearest-neighbor direction is oriented in parallel with the applied electric field compared to any other orientation within the same plane. Specifically, the PbS NCs were found to assemble in a superlattice with hexagonal close-packed structure oriented with the [0001] direction normal to the substrate. In this structure, the nearest-neighbor direction is one of the family of the $\{2\bar{1}\bar{1}0\}$ directions, of which there are six within the (0001) plane at equal angles of 60°. Thus, the maximum deviation from a perfect alignment of the electric field with the nearest-neighbor direction is α = 60°/2 = 30°. All superlattices with α close to 0° exhibited significantly larger (40–50%) electric conductivities than otherwise identical superlattices with α close to 30° (Figure 4).

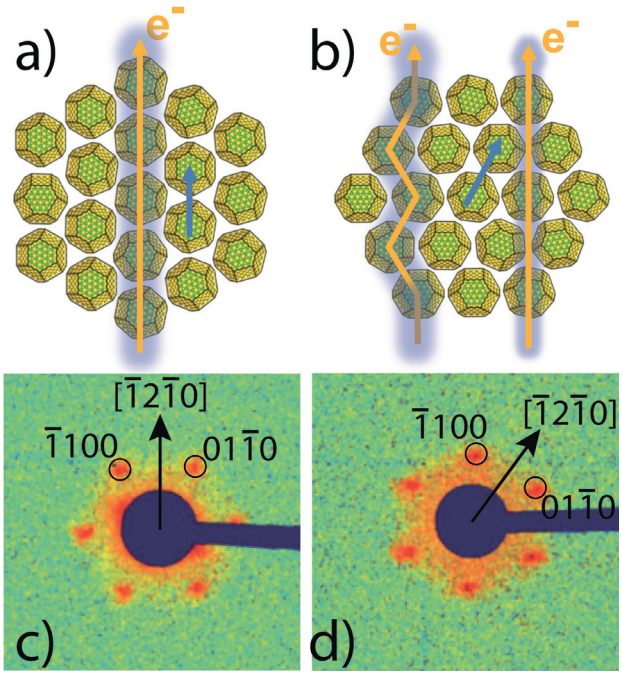

Figure 4. [0001] plane of a hexagonally close-packed superlattice of PbS NCs in two different orientations with respect to the applied electric field, where a) is 40-50% more conductive than b). Corresponding Small angle X-ray diffraction patterns, revealing that in c) the $[\bar{1}2\bar{1}0]$ direction, which is the nearest-neighbor direction, is parallel to the applied electric field, while in d) it is tilted by ~30° to the field.

Another remarkable finding of the same work is that transport is most efficient along the family of {110} directions of the NCs. This is an immediate consequence of the mesocrystalline nature of the superlattice, in which the family of {110} directions of the atomic lattices of the NCs are iso-oriented with the family of the $\{2\bar{1}\bar{1}0\}$ directions of the superlattice. Coincidence or not, this result potentially indicates facet-specific electronic coupling as an additional source for the experimentally observed transport anistotropy in these superlattices. This would be consistent with the theoretical predictions detailed in section 3.

6. ENHANCED ELECTRONIC COUPLING IN SUPERLATTICES OF $Au_{32}(^nBu_3P)_{12}Cl_8$ NANOCLUSTERS

A long-standing fundamental question about charge transport in semiconductor NC ensembles has been the importance of the size inhomogeneity.[24] For crystallites above a certain number of atoms (usually a few 100s), there are various possibilities for adding the next atom to the surface with almost the same (small) change in Gibbs enthalpy. Therefore, such crystallites are never exactly identical, neither in structure nor in the number of atoms, and even the most homogeneous semiconductor NCs of today still exhibit size dispersions of ~4%.[25] Due to the quantum size effect in semiconductor NCs, this structural inhomogeneity results in different energies of the first excited state, which leads to energetic disorder in ensembles of such NCs. With respect to equation (1), the disorder increases and slows down the polaronic hopping rate. A rough theoretical estimate of the impact of this disorder on the expected charge carrier mobility in NC ensembles showed that it can become the dominant limitation of transport and may even prevent highly efficient, band-like transport entirely.[24] First experimental attempts to prove the detrimental effect of energetic disorder were unsuccessful, however, one may argue that coupling in the investigated ensembles was too low to observe the effect.[26]

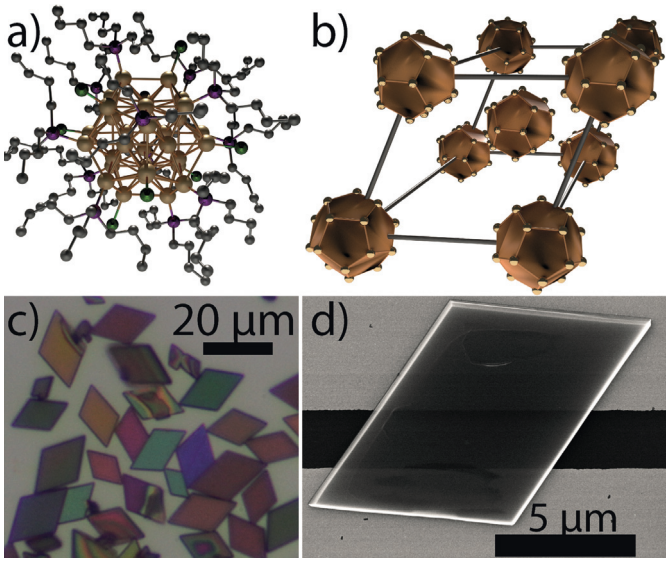

Figure 5. a) Au_{32} nanocluster with peripheral chloride, phosphorus and carbon atoms. Au gold, P purple, Cl green and C grey. (Adapted with permission from ref. [29]. Copyright (2019) WILEY-VCH.) b) Schematic drawing of the triclinic unit cell of the superlattice after self-assembly. Ligand spheres are omitted for clarity. c) Optical micrograph of self-assembled Au_{32}-NC superlattices on a Si/SiOx substrate. Different sizes and thicknesses (color) can be observed. d) SEM micrograph of an individual superlattice deposited on two Au-electrodes on a Si/SiOx device.

A closely related effect to energetic disorder by inhomogeneities of the NCs in a superlattice is the energetic disorder introduced by structural defects in the superlattice itself. Structural defects such as cracks, point-, line- or twinning-defects have been well described for many NC superlattices.[11, 21, 27] They often arise from kinetic arrest during self-assembly under non-equilibrium conditions or due to the afore-mentioned size dispersion of the constituting NCs, which introduces stress to the superlattices. Therefore, it is inherently difficult to distinguish the effect of energetic disorder due to a varying degree of size quantization energy from that due to structural defects, as both effects often appear together.

A recent study on charge transport in ensembles of semiconducting $Au_{32}(^nBu_3P)_{12}Cl_8$ nanoclusters (Figure 5a) has now been successful in quantifying the effect of solely structural disorder.[28] This has become possible owing to the structurally and atomically precise composition of these clusters, which distinguishes them from the larger crystallites with significant size-distribution discussed above.[29] Thus, the energy of the first excited state is identical for all NCs in the ensemble such that the remaining disorder is due to structural defects in the superlattice. Two extremes were compared: poly-crystalline ensembles with mainly short-range order vs. single-crystalline superlattices with near-perfect long-range order and a well-defined superlattice unit cell (Figure 5b). The key result of this comparison is that the electric conductivity is two orders of magnitude higher in the single-crystalline superlattices (for examples of single superlattices see Figure 5c-d). This could be correlated with a vanishing degree of energetic disorder in the superlattice, in contrast to the polycrystalline ensemble for which a significant degree of energetic disorder was determined.

7. OUTLOOK

What is the value of long-range order and orientation for transport in NC superlattices? Similar to an array of atoms, transport through an array of NCs becomes drastically more efficient if it exhibits a large degree of long-range structural order. Current materials that show this effect are in the weak electronic coupling regime. In this regime, transport through the NC superlattice is dominated by the effect of interparticle distance, which leads to the attractive emergent property of anisotropic charge transport. Iso-orientation of the constituting NCs in the superlattice emphasizes facet-specific electronic coupling, which may further increase the anisotropy. The predicted formation of minibands in such NC superlattices as a result of structural order has not been demonstrated, yet, owing to the weak degree of interparticle coupling.[30] To this end, future studies need to excel in realizing even stronger electronic coupling in such NC superlattices beyond the degree of the materials briefly summarized here.

8. ACKNOWLEDGEMENTS

Financial support of this work has been provided by the Emmy Noether program of the DFG under grant SCHE1905/3-1. Andre Maier is acknowledged for a critical review of the manuscript.

9. BIBLIOGRAPHY

[1] C. B. Murray, C. R. Kagan, M. G. Bawendi, *Science* 1995, **270**, 1335–1338.

[2] L. E. Brus, *J. Chem. Phys.* 1983, **79**, 5566–5571.

[3] a) E. V. Shevchenko, D. V. Talapin, N. A. Kotov, S. O'Brien, C. B. Murray, *Nature* 2006, **439**, 55–59; b) M. Nagel, S. G. Hickey, A. Frömsdorf, A. Kornowski, H. Weller, *Z. Phys. Chem.* 2007, **221**, 427–437 c) Z. Fan, M. Grünwald, *J. Am. Chem. Soc.* 2019, **141**, 1980-1988; d) M. A. Boles, M. Engel, D. V. Talapin, *Chem. Rev.* 2016, **116**, 11220–11289.

[4] W. Chen, J. Zhong, J. Li, N. Saxena, L. P. Kreuzer, H. Liu, L. Song, B. Su, D. Yang, K. Wang et al., *J. Phys. Chem. Lett.* 2019, **10**, 2058–2065.

[5] P. Liljeroth, K. Overgaag, A. Urbieta, B. Grandidier, B. Grandider, S. G. Hickey, D. Vanmaekelbergh, *Phys. Rev. Lett.* 2006, **97**, 1–4.

[6] A. P. Kaushik, B. Lukose, P. Clancy, *ACS Nano* 2014, **8**, 2302–2317.

[7] C.-S. Tan, H.-S. Chen, C.-Y. Chiu, S.-C. Wu, L.-J. Chen, M. H. Huang, *Chem. Mater.* 2016, **28**, 1574–1580.

[8] N. Yazdani, S. Andermatt, M. Yarema, V. Farto, M. H. Bani-Hashemian, S. Volk, W. Lin, O. Yarema, M. Luisier, V. Wood, arxiv preprint 2019: https://arxiv.org/abs/1909.09739.

[9] M. V. Kovalenko, M. Scheele, D. V. Talapin, *Science* 2009, **324**, 1417–1420.

[10] S. Shaw, B. Yuan, X. Tian, K. J. Miller, B. M. Cote, J. L. Colaux, A. Migliori, M. G. Panthani, L. Cademartiri, *Adv. Mater.* 2016, **28**, 8892–8899.

[11] B. T. Diroll, X. Ma, Y. Wu, C. B. Murray, *Nano. Lett.* 2017, **17**, 6501–6506.

[12] a) A. André, C. Theurer, J. Lauth, S. Maiti, M. Hodas, M. Samadi Khoshkhoo, S. Kinge, A. J. Meixner, F. Schreiber, L. D. A. Siebbeles et al., *Chem. Commun.* 2017, **53**, 1700–1703; b) S. Maiti, S. Maiti, A. Maier, J. Hagenlocher, A. Chumakov, F. Schreiber, M. Scheele, *J. Phys. Chem. C* 2019, **123**, 1519–1526; c) M. Samadi Khoshkhoo, S. Maiti, F. Schreiber, T. Chassé, M. Scheele, *ACS Appl. Mater. Interfaces* 2017, **9**, 14197–14206.

[13] T. Holstein, *Annals of Physics* 1959, **8**, 325–342.

[14] N. Prodanovic, N. Vukmirovic, Z. Ikonic, P. Harrison, D. Indjin, *J. Phys. Chem. Lett.* 2014, **5**, 1335–1340.

[15] R. A. Marcus, *Angew. Chem. Int. Ed.* 1993, **32**, 1111–1121.

[16] I.-H. Chu, M. Radulaski, N. Vukmirovic, H.-P. Cheng, L.-W. Wang, *J. Phys. Chem. C* 2011, **115**, 21409–21415.

[17] D. Zherebetskyy, M. Scheele, Y. Zhang, N. Bronstein, C. Thompson, D. Britt, M. Salmeron, P. Alivisatos, L.-W. Wang, *Science* 2014, **344**, 1380–1384.

[18] H. Cölfen, M. Antonietti, *Angew. Chem. Int. Ed.* 2005, **44**, 5576–5591.

[19] L. Bahrig, S. G. Hickey, A. Eychmüller, *Cryst. Eng. Comm.* 2014, **16**, 9408–9424.

[20] a) I. A. Zaluzhnyy, R. P. Kurta, A. André, O. Y. Gorobtsov, M. Rose, P. Skopintsev, I. Besedin, A. V. Zozulya, M. Sprung, F. Schreiber et al., *Nano Lett.* 2017, **17**, 3511–3517; b) R. Li, K. Bian, T. Hanrath, W. A. Bassett, Z. Wang, *J. Am. Chem. Soc.* 2014, **136**, 12047–12055.

[21] N. Mukharamova, D. Lapkin, I. A. Zaluzhnyy, A. André, S. Lazarev, Y. Y. Kim, M. Sprung, R. P. Kurta, F. Schreiber, I. A. Vartanyants et al., *Small* 2019, **15**, 1904954.

[22] I. A. Zaluzhnyy, R. P. Kurta, M. Scheele, F. Schreiber, B. I. Ostrovskii, I. A. Vartanyants, *Materials* 2019, **12**, 3464.

[23] A. Maier, D. Lapkin, N. Mukharamova, P. Frech, D. Assalauova, A. Ignatenko, R. Khubbutdinov, S. Lazarev, M. Sprung, F. Laible et al., arxiv preprint 2020, https://arxiv.org/abs/2003.03266.

[24] P. Guyot-Sionnest, *J. Phys. Chem. Lett.* 2012, **3**, 1169–1175.

[25] O. Chen, J. Zhao, V. P. Chauhan, J. Cui, C. Wong, D. K. Harris, H. Wei, H.-S. Han, D. Fukumura, R. K. Jain et al., *Nat. Mater.* 2013, **12**, 445–451.

[26] Y. Liu, M. Gibbs, J. Puthussery, S. Gaik, R. Ihly, H. W. Hillhouse, M. Law, *Nano Lett.* 2010, **10**, 1960–1969.

[27] M. I. Bodnarchuk, E. V. Shevchenko, D. V. Talapin, *J. Am. Chem. Soc.* 2011, **133**, 20837–20849.

[28] F. Fetzer, A. Maier, M. Hodas, O. Geladari, K. Braun, A. J. Meixner, F. Schreiber, A. Schnepf, M. Scheele, arxiv preprint 2020, https://arxiv.org/abs/2002.06454.

[29] S. Kenzler, F. Fetzer, C. Schrenk, N. Pollard, A. R. Frojd, A. Z. Clayborne, A. Schnepf, *Angew. Chem. Int. Ed.* 2019, **58**, 5902–5905.

[30] O. L. Lazarenkova, A. A. Balandin, *J. Appl. Phys.* 2001, **89**, 5509–5515.